Domain-wall step motors: Controlling the motion of magnetic domain walls using patterned magnetic films

Sergey Savel'ev,[1,2] A. L. Rakhmanov,[1,3] and Franco Nori[1,4]
[1]*Frontier Research System, The Institute of Physical and Chemical Research (RIKEN), Wako-shi, Saitama 351-0198, Japan*
[2]*Department of Physics, Loughborough University, Loughborough LE11 3TU, United Kingdom*
[3]*Institute for Theoretical and Applied Electrodynamics RAS, 125412 Moscow, Russia*
[4]*Center for Theoretical Physics, Department of Physics, University of Michigan, Ann Arbor, Michigan 48109-1040, USA*
(Received 25 January 2006; revised manuscript received 17 May 2006; published 10 July 2006)

Magnetic domain walls can move when driven by an applied magnetic field. This motion is important for numerous devices, including magnetic recording read/write heads, transformers, and magnetic sensors. A magnetic film with a sawtooth profile localizes magnetic domain walls in discrete positions at the narrowest parts of the film. We propose a controllable way to move these domain walls between these discrete locations by applying magnetic-field pulses. A similarly patterned magnetic film attached to a larger magnetic element at one end of the film can operate as an XOR logic gate.

DOI: 10.1103/PhysRevB.74.024404 PACS number(s): 75.60.Ch, 05.45.−a, 85.70.Kh

I. INTRODUCTION

The very fast growth of information technology requires novel approaches to information storage, control, and manipulation. Most magnetic memory devices store information by setting either up or down the magnetization of small magnetic particles or individual domains in magnetic films (see, e.g., Refs. 1–4). Such systems can be driven either by polarized currents (see, e.g., Refs. 5–9) or by magnetic fields generated by external sources.[3,10]

Nonlinear logical devices (e.g., Refs. 11 and 12) operating at room temperature attract considerable interest[1] because these do not require expensive cryogenics (in contrast to superconducting devices). In this context, here we focus on a domain wall moving through a periodically patterned film and driven by magnetic-field pulses. This motion can be mapped to the motion of an overdamped particle within a wide range of parameters, which covers many possible applications.[13] Recently, the motion of tiny particles in periodic ratchetlike potentials has inspired a new generation of solid-state devices[14–22] and here we study how these ideas could be used for magnetic thin films. Magnets with constrictions[23–31] or triangles[22,26,27,32,33] are currently being actively studied by different groups because these provide very attractive features over more conventional structures.

We propose setups for controllable magnetic domain-wall step motors and logic gates using sawtooth-shaped ferromagnetic slabs or films. The precise and controllable discrete motion of domain walls in these structures (Fig. 1) can be achieved by applying magnetic-field pulses (Fig. 2). Moreover, a chain of identical magnetic "teeth" attached to a larger magnetic element (Fig. 3) can operate as a logic gate somewhat reminiscent of a cellular automata[12] made of a chain of magnetic particles.

A step motor is a device where some input signal is processed to accomplish an end result, typically controlled motion. Thus, we propose a step motor that controls the motion of magnetic domain walls (MDW) in a patterned magnetic slab. Like standard step motors, ours can be precisely controlled, so that the MDW can move a desired number of "steps." Also, in standard step motors, each input electrical pulse produces one increment or step (thus the name step motor). In our proposal, each applied magnetic pulse can produce one increment or step motion for a MDW. This could be useful for the design of shift registers if local magnetic fields could be independently applied to each magnetic tooth (Fig. 1). Longer or stronger applied magnetic pulses can produce MDW motion involving a controlled number of steps. Other devices were also studied in Ref. 11, and another geometry is also considered in Ref. 34. After this work was initially submitted, a related experimental system appeared in Ref. 32, vindicating our initial proposal as both experimentally relevant and of interest.

II. MODEL

We consider a soft ferromagnetic slab or film patterned with many triangles in the sawtooth shape shown in Fig. 1(a). Here we assume the triangles to be isosceles (i.e., symmetric sawtooth). It is easy to extend our results to ratchet-type nonsymmetric sawteeth. We assume that the easy axis (z axis in Fig. 1) for the magnetization lies in the film plane and is perpendicular to the x axis in Fig. 1. We also assume that the magnetic anisotropy field H_a is not small, in order to minimize the alignment of the magnetization along the sample side surface. In particular, the thickness of the layer δ_1 near the surface, where magnetization vector deflects from the direction of the easy axis, is small compared to the characteristic scale x_0 of the sawtooth structure. In this case, if the sawtooth profile is sufficiently elongated (see Fig. 1), the magnetization vector would be aligned along the easy axis in most of the sample volume, and domain walls should also be parallel to this axis. The corresponding limitation on H_a will be presented below. Such a structure (which meets our assumptions) can be manufactured by standard techniques.[1]

The linear energy density $E(x)$ of the film in the externally applied magnetic field $H_e(t)$ along the z direction (see Fig. 1) can be written as

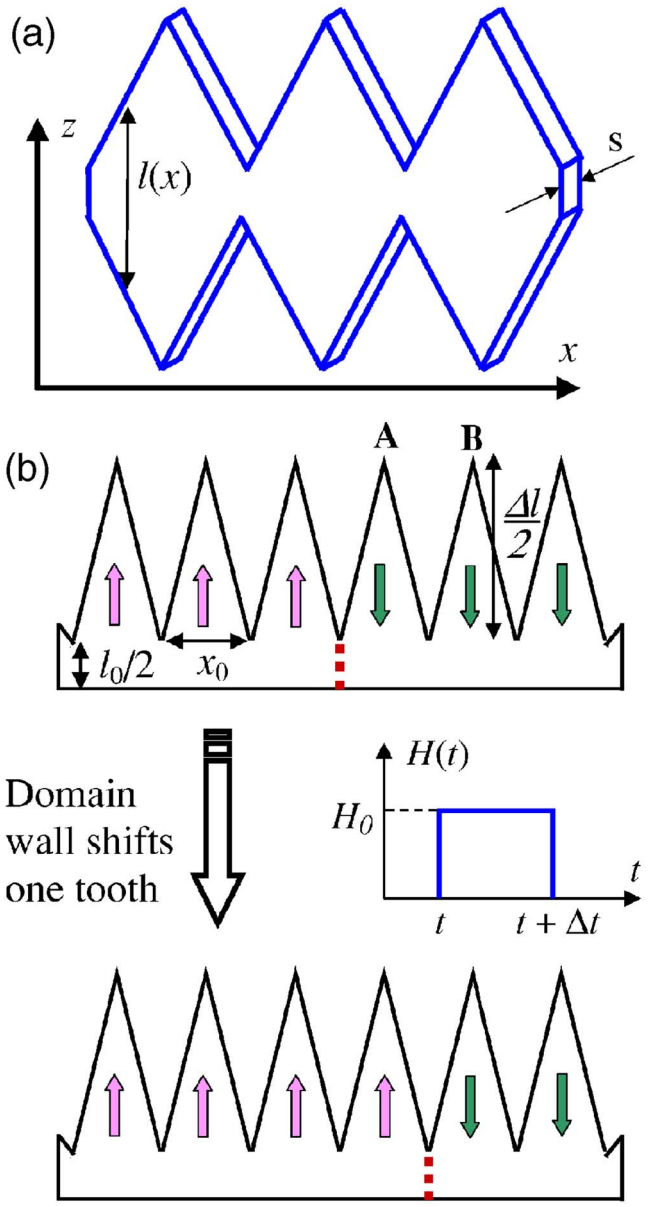

FIG. 1. (Color online) (a) 3D sketch of the sample, indicating the height $l(x)$ and width s. Since the sample is mirror-symmetric along the x direction, hereafter we only draw the top part, to save space. (b) Schematic diagram of a magnetic domain wall (red dashed vertical line) moving in a triangular-patterned film (here we only show its upper half). The magnetic domain wall separates regions having different orientations of the magnetization (shown by the up and down arrows). This wall can be shifted from one minimum-thickness location to another one by applying an external magnetic-field pulse. This domain-wall motion is easily controllable and robust to small variations of the magnetic-field pulse, e.g., possible errors in either the duration Δt or the amplitude H_0 of the pulses (see text). These pulses can be generated by an external solenoid magnet (not shown here).

$$E(x) = E_W l(x) s - 2MH_e(t) s \int_0^x l(x')dx' + E_{\text{str}}, \qquad (1)$$

where x is the location of the domain wall, E_W is its energy per unit area, $l(x)$ is the variable film width, s is the constant

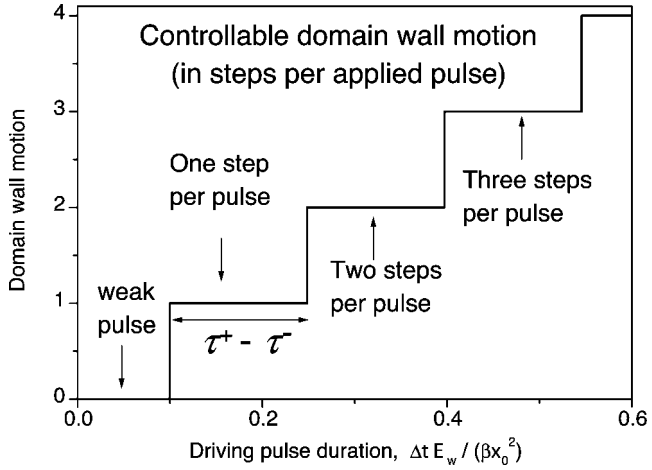

FIG. 2. Controllable discrete shift of a domain-wall location vs the duration of the applied driving pulse, calculated using Eqs. (7) and (10). The long flat plateaus indicate the robustness of the proposed magnetic domain-wall step motor to errors in the applied pulse time Δt and intensity h_0.

film thickness, M is the film magnetization, and E_{str} is the stray field contribution. The second term on the right-hand side of Eq. (1) is the usual Zeeman energy. The energy E_W of the domain wall can be expressed as

$$E_W = 4\pi\gamma M^{3/2} H_a^{1/2} l_{\text{exchange}}, \qquad (2)$$

where $\gamma \sim 1$ and l_{exchange} is the exchange length. The approximations discussed here have been successfully used[13] for describing magnetic domain-wall motion in different systems. When the length x_0 of each tooth decreases, the domain-wall thickness $\delta \sim l_{\text{exchange}}\sqrt{M/H_a}$ could approach the characteristic scale x_0 of the sawtooth, resulting in the renormalization[31] of δ and E_W. However, for standard materials and micrometer-sized tooth sizes, the domain-wall thickness is much less than x_0, i.e., $\delta \ll x_0$. Note that the thickness δ_1 of the surface layer, in which the magnetization vector deflects from the easy-axis direction, is of the order of the domain-wall thickness δ (see the Appendix). As a result, the conditions $\delta \ll x_0$ and $\delta_1 \ll x_0$ limit the anisotropy field. These conditions can be written in the form

$$H_a \gg M \frac{l_{\text{exchange}}^2}{x_0^2}. \qquad (3)$$

This last inequality is valid for all our estimates. Indeed, below we estimate $\delta \sim 0.03\ \mu\text{m} \ll x_0 \sim 1\ \mu\text{m}$. Thus, Eq. (1) should be applicable for our problem, at least qualitatively. A more realistic study would require detailed micromagnetic simulations, which are beyond the scope of this paper.

The external magnetic field $H_e(t)$ drives the wall in the patterned metal film according to the usual dynamical equation: (Friction force) $= -dE(x)/dx$. For simplicity, we neglect the contribution to the total force due to stray magnetic fields. As shown in the Appendix, the stray field term can be neglected in the case of soft magnetic materials, $H_a \ll M$, which is of most interest for the present study. Thus, the equation of motion for the MDW can be rewritten as

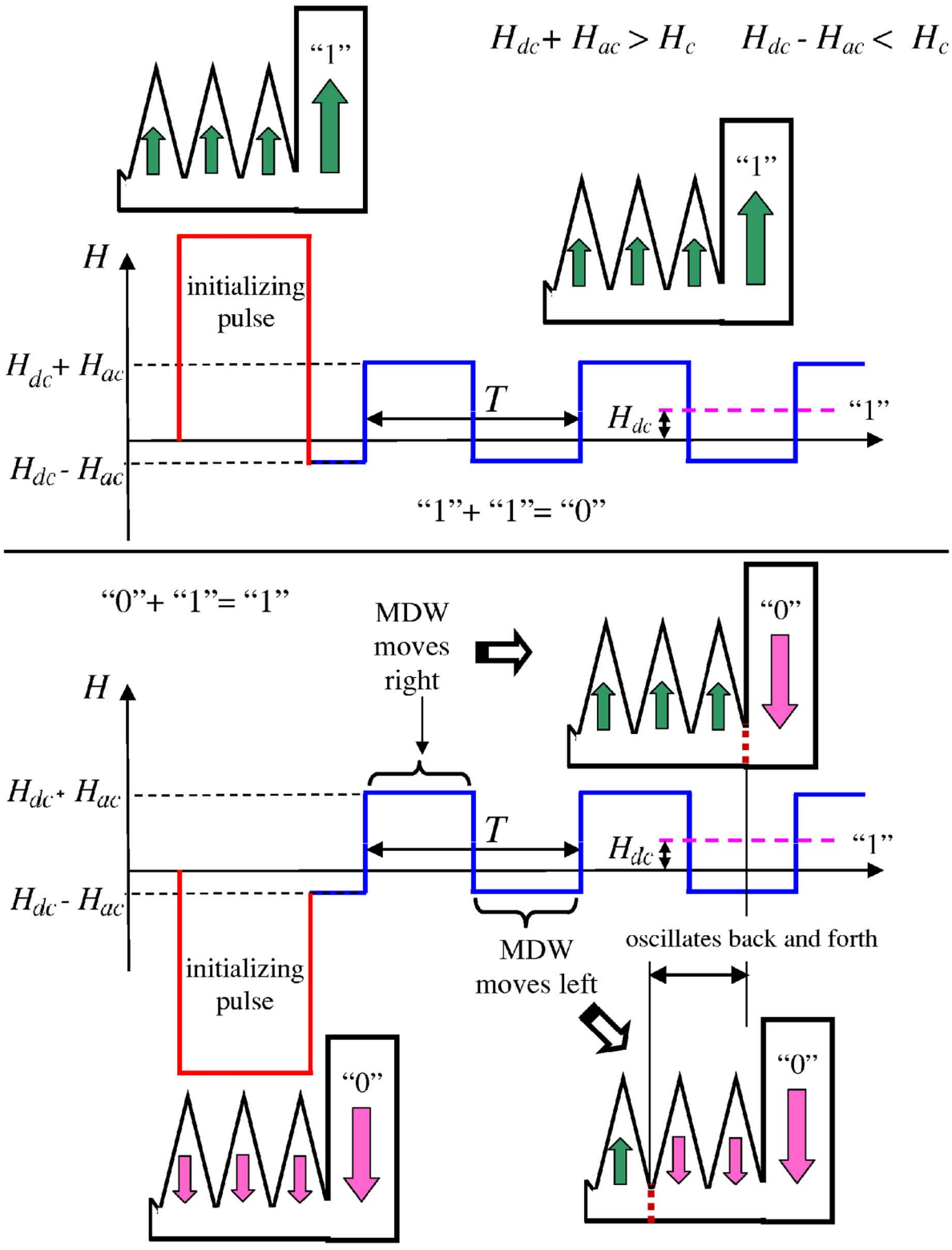

FIG. 3. (Color online) Schematic diagram of a magnetic logic gate. When applying a magnetic field, the entire patterned magnetic sample can be set to either its "0" or "1" state. This structure can work as an XOR gate if both ac and dc magnetic fields are applied: $H_{dc}+H_{ac}(t)$. The inputs of the XOR gate are (i) an applied dc field and (ii) the magnetization of the larger part of the structure. Then an ac field is added to start the XOR operation. The output can be either 0 (no domain wall) or 1 (a domain wall is nucleated in the sample and oscillates). This MDW oscillation corresponds to the "1" output state and can generate a voltage in a pick-up coil. Thus, the moving domain wall exists either for $H_{dc}<0$ and state "1" or $H_{dc}>0$ and state "0."

TABLE I. Comparison between magnetic domain-wall (MDW) motion in constrictions and the motion of an overdamped particle.

	Magnetic Domain Wall (MDW)	Overdamped particle
Model	$\dot{\chi}=-l'(\chi)/l(\chi)+h(t)-f_p\dot{\chi}/\lvert\dot{\chi}\rvert$	$\dot{x}=-u'+f(t)$
Viscous friction	Yes	Yes
Static friction	Yes due to pinning	No
Inertia	Only at high frequencies	No
Potential due to	(periodic) constrictions, $l(x)$ (e.g., sawtooth shape of magnetic film)	Substrate, $u(x)$
ac drive due to	externally applied ac magnetic field $h(t)$	ac force $f(t)$
Ratchet effect (dc transport from ac drive) when	asymmetric shape of periodic constrictions (e.g., asymmetric sawtooth shape of magnetic film)	asymmetric ratchet potential[14,19]
dc transport for time asymmetric drive (harmonic mixing) when	symmetric constriction, but time-asymmetrically changing magnetic field, e.g., $h(t)=h_0\cos\omega t+h_1\cos(2\omega t+\phi)$ (transport controlled by ϕ)	symmetric potential, but the driving force is asymmetric in time (see, e.g., Ref. 36), e.g., $f(t)=f_0\cos(\omega t)+f_1\cos(2\omega t+\phi)$ (transport controlled by ϕ)
Diffusion enhancement when	dc magnetic field pushes the wall to the transition from trapped (between constrictions) to running motion	Driving force pushes the system close to the transition from trapped to running motion[37]
Weak signal amplification via either stochastic resonance[38] or deterministic signal mixing[39]	Yes	Yes

$$\beta\dot{x}=-\frac{E_W}{l(x)}\frac{dl(x)}{dx}+2MH_e(t)-F_{\rm pin}\frac{\dot{x}}{|\dot{x}|}\quad \text{for } \dot{x}\neq 0. \tag{4}$$

Here, $\dot{x}=dx/dt$. The friction force per unit area acting on the wall comes from two contributions:[13] (i) the eddy current friction, $\beta\dot{x}l(x)$, with $\beta=\gamma_1(2\pi M)^2/\rho c^2$, and (ii) the domain-wall "pinning" force, $-F_{\rm pin}\dot{x}/|\dot{x}|$. Here, ρ is the film's electrical resistivity and γ_1 is a constant of the order of unity which depends on the sample geometry. The pinning force can be written as $F_{\rm pin}=MH_{\rm pin}$, where $H_{\rm pin}$ refers to the pinning field. The pinning force arises due to inhomogeneities of the magnetic properties of the sample, such as structural defects, crystal grain boundaries, inclusions, and geometrical imperfections.[35] In Eq. (4), we omit the inertia term: this is usually valid up to several tens of GHz. In dimensionless units, Eq. (4) is reduced to

$$\dot{\mathcal{X}}=-\frac{l'(\mathcal{X})}{l(\mathcal{X})}+h(t)-f_p\frac{\dot{\mathcal{X}}}{|\dot{\mathcal{X}}|}, \tag{5}$$

where $\mathcal{X}=x/x_0$, $\dot{\mathcal{X}}=d\mathcal{X}/d\tau$, $\tau=t/t_0$, $'=d/d\mathcal{X}$, $h(t)=2MH_e(t)x_0/E_W$, and $f_p=F_{\rm pin}x_0/E_W$. Here, the spatial scale x_0 is the period of sawtooth structure (Fig. 1) and $t_0=\beta x_0^2/E_W$ is the characteristic damping time.

Thus, a magnetic domain wall moving in the patterned ferromagnetic slab or film can be described by Eq. (5), i.e., the motion of a MDW can be mapped into the motion of an overdamped particle. This offers a powerful analogy (described in Table I) since the transport and diffusion properties of a single overdamped particle have been studied for decades and some of these results could be used to better explore the dynamics of MDWs in constrictions.

III. CONTROLLABLE DOMAIN-WALL STEP MOTOR

Under steady-state conditions, the magnetic domain walls in the film shown in Fig. 1 can only be located at certain discrete positions, corresponding to the narrowest parts of the patterned film (e.g., red dashed lines in Fig. 1). This would occur if the sawtooth profile is steep enough in order for the restoring force (per unit area) to overcome the pinning force, $|l'(\mathcal{X})|/l(\mathcal{X})>f_p$. When the driving magnetic-field pulse $H(t)$ shown in Fig. 1 is applied, the domain wall can be shifted from one minimum-thickness position to another one. For a rectangular pulse of the applied magnetic field, Eq. (5) can be integrated exactly. This allows us to derive the times, τ^+ and τ^-, for the transitions of the domain wall from a minimum to the following maximum (τ^+) and from a maximum to the following minimum (τ^-):

$$\tau^{\pm} = \int_0^{1/2} \frac{d\mathcal{X}}{h_0 - f_p \mp l'(\mathcal{X})/l(\mathcal{X})}. \quad (6)$$

Here, we introduce the dimensionless pulse amplitude $h_0 = 2MH_0x_0/E_W$. The symmetric-shape assumption was used for the first time in Eq. (6). Hereafter, $\tilde{h} \equiv h_0 - f_p$ (=driving-pinning) denotes the "effective depinning drive." Strictly speaking, the assumption of a piecewise-linear structure (isosceles-triangles) profile is only needed from this point. For a piecewise-linear structure, shown in Fig. 1, these transition times can be explicitly written as

$$\tau^{\pm} = \frac{1}{2\tilde{h}} \pm \frac{1}{\tilde{h}^2} \ln\left[1 + \frac{\tilde{h}\Delta l}{\tilde{h}l_0 \mp 2\Delta l}\right], \quad (7)$$

where we use the expression

$$l(\mathcal{X}) = l_0 + 2\mathcal{X}\Delta l \quad \text{for } \mathcal{X} < 1/2 \quad (8)$$

(i.e., from the minimum to the following maximum of the sawtooth profile). The domain wall cannot be shifted from its initial position if the dimensionless magnetic-field pulse $h(t)$ has an amplitude h_0 smaller than the threshold value,

$$h_{\text{onset}} = f_p + \frac{2\Delta l}{l_0}. \quad (9)$$

At stronger pulses, the wall can be shifted any desired number N of steps by changing the duration Δt of the pulse (Fig. 2),

$$N\tau^+ + (N-1)\tau^- < \Delta t < (N+1)\tau^+ + N\tau^-. \quad (10)$$

It is important to emphasize the robustness of this controllable step motor: due to the discrete equilibrium positions of the domain wall, we can shift it *an exact integer number of steps, even though the pulse duration is established within an accuracy of about* $(\tau^+ - \tau^-)$.

Let us consider a MDW in the potential minimum shown by the red dashed line in Fig. 1(b). If the applied $H_e(t)$ pulse drives the MDW below the (potential energy) maximum marked by "A," then the MDW returns to its original position. If the applied $H_e(t)$ pulse drives the MDW beyond "A," but before the next maximum "B," then the MDW reaches the next minimum of energy. This means that *two out of three* consecutive linear segments of the profile *automatically* bring the MDW to the next minimum. This makes the device quite robust, since there is no need to very-fine-tune the applied pulse $H_e(t)$ to reach the next "step" in the step motor.

Obviously, for homogeneous magnetic materials, the dimensionless pinning force f_p is less than 1. In this case, the threshold amplitude h_{onset} of the magnetic pulse is determined by the sawtooth geometry. For rough estimates, we take standard parameter values. For instance, for permalloy films, $M \sim 1$ kOe, $H_a \sim 10$ Oe, $l_{\text{exchange}} \sim 3$ nm, $x_0 \sim 1$ μm, $\Delta l/l_0 \sim 5$, and $\rho \sim 1$ $\mu\Omega$m. This gives $\delta \sim 30$ nm $\ll x_0$, $t^{\pm} \sim 10$ μs, and $H_{\text{onset}} \sim H_{\text{pin}} + 1.5$ Oe. The pinning field is a property of the specific magnetic material and its preparation. In some cases, it could be estimated. For example, following Ref. 41 (for the domain-wall pinning on planar defects characterized by a lower magnetic anisotropy field $\tilde{H}_a$), we find $H_{\text{pin}}/H_a \approx 1 - \tilde{H}_a/H_a$. An analogous estimate for a film with geometrical imperfections provides $H_{\text{pin}} \approx H_a(\Delta d/d)$ (here Δd is the characteristic roughness of the film thickness). Note that it is easy to prepare samples with the pinning field lower than several Oe. When increasing the pulse amplitude, additional domain walls can penetrate from the open ends of the structure. For homogeneous materials this occurs for $H > H_c \sim H_a$, where H_c is the critical field for nucleating a domain wall.

IV. LOGIC GATES

The nucleation and propagation of domain walls in the patterned sawtooth film can be used for the design of logic devices.[11,12] Here we propose the asymmetric magnetic structure shown in Fig. 3: a larger (e.g., rectangular) element is attached to one of the ends of the sawtooth structure. Using this device, we can construct an XOR logic gate. Although not shown in Fig. 3, the magnetic wall XOR gate includes the solenoid magnet for applying pulses of an external magnetic field in order to magnetize this magnetic structure as well as to nucleate and move the magnetic domain wall.

The initialization and operation of this gate are shown in Fig. 3. Namely, the large pulse of the externally applied magnetic field magnetizes the whole structure either up or down. When the whole magnetic structure is magnetized upward, it is a logic state "1," and when the whole structure is magnetized downward, it is a logic state "0" (see Fig. 3 and Table II). Next, we combine both the zero average ac field $H_{\text{ac}}(t)$ and a dc bias field H_{dc}. For instance, let us consider rectangular ac pulses with temporal period T: $H_{\text{ac}}(t) = H_{\text{ac}}(t+T)$,

$$H_{ac}(t) = H_0 \quad \text{for } t < T/2 \text{ and}$$

$$H_{\text{ac}}(t) = -H_0 \quad \text{for } t > T/2. \quad (11)$$

It is possible to assign another state, that is, "1" for H_{dc} directed up and "0" for H_{dc} directed down (see Fig. 3 and Table II). We can always choose an ac signal so that $H_0 > |H_{\text{dc}}|$ and $H_0 - |H_{\text{dc}}| < H_c < H_0 + |H_{\text{dc}}|$, where H_c is the threshold field for domain-wall nucleation at the open end of the sawtooth structure. Due to strong shape anisotropy, the magnetization reversal field H_{c1} of the large attached element is higher than both H_c and $H_0 + |H_{\text{dc}}|$.

If both states coincide ("1" + "1") or ("0" + "0"), the magnetization reversal process does not occur (output is "0") (see Fig. 3 and Table II). Indeed, when the ac magnetic-field direction is opposite to the direction of the film magnetization, the total field $H_0 - |H_{\text{dc}}|$ is not enough to create a domain wall at the open end (i.e., the whole magnetic structure is magnetized either up or down during an XOR operation and there is no domain wall).

For the cases when ("1" + "0") or ("0" + "1"), the dc field assists the ac field $(H_0 + |H_{\text{dc}}|)$ to nucleate a domain with opposite magnetization with respect to the magnetization of the larger element. Therefore, when both states are different, ("1" + "0") or ("0" + "1"), the nucleated domain wall

TABLE II. Inputs and output of the domain-wall XOR gate. The domain-wall motion reveals that the two inputs were different. No domain wall implies that the two inputs were equal.

Input A	Input B	Output
magnetization of large element: upward for "1" downward for "0"	dc magnetic field H_{dc} up $H_{dc}>0$ for "1" down $H_{dc}<0$ for "0"	domain-wall motion oscillates for "1" no domain wall for "0"
0	0	0
1	1	0
0	1	1
1	0	1

moves back and forth inside the structure. This produces a magnetic response attributed to a new state "1" (see Fig. 3 and Table II) and could be measured (e.g., by pick-up coils). The amplitude of the output signal depends on the duration of the ac pulses. Thus, this device operates as an XOR logic element.

V. CONCLUSIONS

We propose ways to precisely control the motion of domain walls in patterned magnetic films. These could be used for making controllable step motors moving domain walls and for logic gates. Our estimates indicate that these devices can be made from rather standard magnetic materials using conventional technology. These devices can operate at room temperature since thermal noise is negligible with respect to their characteristic energies.

ACKNOWLEDGMENTS

We acknowledge useful conversations with Y. Otani, O. Fruchart, and G. Tatara. This work was supported in part by the LPS, ARO, National Security Agency (NSA) and Advanced Research and Development Activity (ARDA) under Air Force Office of Research (AFOSR) Contract No. F49620-02-1-0334; and also supported by U.S. National Science Foundation Grant No. EIA-0130383. S. S. acknowledges support from the Ministry of Science, Culture and Sports of Japan via the Grant-in-Aid for Young Scientists No. 18740224 and also from EPSRC.

APPENDIX

The stray-fields energy, E_{str}, can be estimated using methods from Refs. 13 and 40. Following Ref. 40, we introduce the potential φ of the stray magnetic field, which obeys the Laplace equation

$$\nabla^2\varphi = 0 \tag{A1}$$

with the boundary conditions at the sample edges

$$-\left(\frac{\partial\varphi}{\partial n}\right)_{+0} + \left(\frac{\partial\varphi}{\partial n}\right)_{-0} = 4\pi M_n, \tag{A2}$$

where $(\partial/\partial n)_{\pm 0}$ means normal to the surface derivative over and under the surface, respectively. The stray energy is

$$E_{str} = \frac{1}{2}\int_S dS M_n\varphi. \tag{A3}$$

The integration is performed over the sample surface S.

This calculation requires the value of the normal to the surface component of the magnetization vector, M_n. In general, this value is a function of the coordinate over the sample surface and should be found using a minimization of the total energy functional (1). However, we assume M_n to be constant and the appropriate value will be estimated below. We neglect the contribution to E_{str} from the film side surfaces and from the sample ends assuming that M_n is negligible over these surfaces since both the anisotropy axis and the external field are along the z direction.

The problem is linear and we can separate the potential φ into a sum of contributions from each sawtooth edge, $\varphi = \Sigma_i\varphi_i$. The normal component of the magnetization at each edge, M_{ni}, is plus or minus $|M_n|$ depending on the domain-wall position. The edge that is crossed by the domain wall is treated as two shorter edges with a different sign of M_{ni}. Each potential φ_i is the solution of the standard boundary problem (A1) and (A2) with $M_n = \pm|M_n|$. Using a Green's function approach for the Laplace equation, we find

$$\varphi_i(\xi_i,\eta_i,z) = -\frac{M_{ni}}{2}\int_0^{\xi_{i1}} d\xi_i' \int_0^s dz' \frac{1}{\sqrt{(\xi_i-\xi_i')^2+(z-z')^2+\eta_i^2}}, \tag{A4}$$

where we introduce the coordinates (ξ_i,η_i) along and transverse each sawtooth edge. The integration in Eq. (A4) is performed over the corresponding edge. Then, by shifting and rotating the coordinate planes (ξ_i,η_i,z), we transform them to the common coordinate system (x,y,z), and find for the stray fields energy

$$E_{str} = -\frac{1}{4}\Sigma_{i,j}M_{ni}M_{nj}\int_{S_j} dS_j\varphi_i(S_j). \tag{A5}$$

The integration is performed over each edge surface S_j.

Using the last formula, we can present the contribution to the force acting on the domain wall due to the stray fields, $f_{str} = -\partial E_{str}/\partial x$, in the form

$$f_{\mathrm{str}} = \frac{M_n^2 s^2}{2\cos\theta} J(x,\theta), \tag{A6}$$

where $\theta = \arctan(\Delta l / x_0)$ is the angle between the sawtooth edge and the x axis, and $J(x,\theta)$ is a dimensionless function. This function was calculated numerically using Eqs. (A4) and (A5), and the coordinate transformation procedure described above. As a result, we find that $J(x,\theta)$ is approximately logarithmic with x, and is zero if the domain wall is in the middle of the sample. This result is natural. Also, if $\theta = 0$, then the sample is a plane strip and, in this case, the problem can be solved analytically,

$$f_{\mathrm{str}} \approx \frac{M_n^2 s^2}{2} \ln\left(\frac{L-x}{x}\right), \quad x^2, (L-x)^2 \gg s^2,$$

where L is the total sample length. Zero force corresponds to an optimal domain configuration. Now we should estimate the normal to the surface magnetization component M_n. This value is quite different for hard and soft ferromagnetic materials.

Consider the magnetization distribution near the sample edge. To reduce the stray field energy, the magnetization vector deflects from the direction of the easy axis within some region of the thickness δ_1 near the surface. Following Ref. 40, the value of M_n can be found by minimization of the sum of the stray, anisotropy, and the exchange magnetic energies in the layer δ_1. Omitting numerical factors, the surface energy per unit area can be estimated as

$$E_{\mathrm{sur}} = M_n^2 s - M H_a \delta_1 \cos^2\psi + \left(\frac{\partial \mathbf{M}}{\partial z}\right)^2 l_{\mathrm{exchange}}^2 \delta_1, \tag{A7}$$

where ψ is the angle between the easy axis and the magnetization vector $\mathbf{M}$. The value of the angle ψ is determined by $M_n = M\cos(\theta+\psi)$, and we replace $(\partial \mathbf{M}/\partial z)^2$ by the approximate value $[(M\cos\theta - M_n)/\delta_1]^2$.

It can be verified that in the case of a hard ferromagnetic sample, when $H_a \geqslant M$, then $\cos\psi = 0$ and $M_n = M\cos\theta$. In this case, the stray fields force is $f_{\mathrm{str}} \approx M^2 \cos\theta s^2 g(x,\theta)/2$, where g is a slowly varying function of the order of 1. The stray fields contribution to the total force acting on the MDW can be neglected if $|E_W\, s(\partial l/\partial x)| \geqslant |f_{\mathrm{str}}|$ or

$$\frac{\sin\theta}{\cos^2\theta} \geqslant \frac{1}{8\pi}\left(\frac{M}{H_a}\right)^{1/2} \frac{s}{l_{\mathrm{exchange}}}, \quad H_a \geqslant M. \tag{A8}$$

The last inequality could be fulfilled if the sample thickness is not large and the angle θ is not small. For example, for $H_a = M$ and $s/l_{\mathrm{exchange}} = 10^3$ the inequality (A8) is valid if $\theta \leqslant 80°$.

In the case of a soft ferromagnet, when $H_a \ll M$, the value of M_n becomes much less than M. Assuming that the angle θ is not very small, the minimization of the value E_{sur} in Eq. (A7) gives

$$M_n \approx \left(M H_a \frac{l_{\mathrm{exchange}}}{s}\right)^{1/2}. \tag{A9}$$

The condition $|E_W\, s(\partial l/\partial x)| \geqslant |f_{\mathrm{str}}|$ now reads

$$\tan\theta \geqslant \frac{1}{8\pi}(H_a/M)^{1/2}, \quad H_a \ll M. \tag{A10}$$

Thus, we can neglect the stray fields contribution for soft ferromagnetic samples. Note that taking into account the y component of the magnetization vector could only reduce the stray fields term. The thickness of the surface region δ_1 is of the order of the domain-wall thickness δ. This means that the proposed approach is valid if Δl and x_0 are greater than δ.

[1] C. D. Mee and E. D. Daniel, *Magnetic Storage Handbook* (McGraw-Hill, New York, 1996).
[2] H. Koo, C. Krafft, and R. D. Gomez, Appl. Phys. Lett. **81**, 862 (2002).
[3] T. Gerrits, H. A. M. van den Berg, J. Hohlfeld, L. Bar, and T. Rasing, Nature (London) **418**, 509 (2002).
[4] H. Boeve, J. Das, C. Bruynseraede, J. De Boeck, and G. Borghs, J. Appl. Phys. **85**, 4779 (1999).
[5] T. Kimura, Y. Otani, K. Tsukagoshi, and Y. Aoyagi, J. Appl. Phys. **94**, 7947 (2003).
[6] T. Kimura, Y. Otani, I. Yagi, K. Tsukagoshi, and Y. Aoyagi, J. Appl. Phys. **94**, 7266 (2003).
[7] Y. Jiang, T. Nozaki, S. Abe, T. Ochiai, A. Hirohata, N. Tezuka, and K. Inomata, Nat. Mater. **3**, 361 (2004).
[8] A. Yamaguchi, T. Ono, S. Nasu, K. Miyake, K. Mibu, and T. Shinjo, Phys. Rev. Lett. **92**, 077205 (2004).
[9] G. Tatara and H. Kohno, Phys. Rev. Lett. **92**, 086601 (2004).
[10] E. Saitoh, M. Kawabata, K. Harii, H. Miyajima, and T. Yamaoka, J. Appl. Phys. **95**, 1986 (2004).
[11] D. A. Allwood, G. Xiong, C. C. Faulkner, D. Atkinson, D. Petit, and R. P. Cowburn, Science **309**, 1688 (2005).
[12] R. P. Cowburn and M. E. Welland, Science **287**, 1466 (2000).
[13] A. G. Gurevich and G. A. Melkov, *Magnetization Oscillations and Waves* (CRC Press, Boca Raton, FL, 1996).
[14] P. Reimann, Phys. Rep. **361**, 57 (2002).
[15] R. D. Astumian and P. Hänggi, Phys. Today **55**(11), 33 (2002).
[16] H. Linke, Appl. Phys. A **75**, 167 (2002), special issue on Brownian motors.
[17] J. F. Wambaugh, C. Reichhardt, C. J. Olson, F. Marchesoni, and F. Nori, Phys. Rev. Lett. **83**, 5106 (1999).
[18] B. Y. Zhu, F. Marchesoni, and F. Nori, Phys. Rev. Lett. **92**, 180602 (2004); Physica E (Amsterdam) **E18**, 318 (2003).
[19] P. Hänggi, F. Marchesoni, and F. Nori, Ann. Phys. **14**, 51 (2005).
[20] S. Savel'ev, F. Marchesoni, and F. Nori, Phys. Rev. Lett. **91**, 010601 (2003); **92**, 160602 (2004); Phys. Rev. E **70**, 061107 (2004); **71**, 011107 (2005); Physica C **388**, 661 (2003); S. Savel'ev, F. Marchesoni, P. Hänggi, and F. Nori, Europhys. Lett. **67**, 179 (2004); Eur. Phys. J. B **40**, 403 (2004); Phys. Rev. E **70**, 066109 (2004); S. Savel'ev and F. Nori, Chaos **15**, 026112 (2005). F. Nori and S. Savel'ev, Physica C **437–438**, 226 (2006).
[21] S. Savel'ev and F. Nori, Nat. Mater. **1**, 179 (2002); D. Cole, S.

Bending, S. Savel'ev, A. Grigorenko, T. Tamegai, and F. Nori, *ibid.* **5**, 305 (2006); A. Tonomura, *ibid.* **5**, 257 (2006); D. Cole, J. S. Neal, M. R. Connolly, S. J. Bending, S. Savel'ev, F. Nori, M. Tokunaga, and T. Tamegai, Physica C **437–438**, 52 (2006).

[22] J. E. Villegas, S. Savel'ev, F. Nori, E. M. Gonzalez, J. V. Anguita, R. García, and J. L. Vicent, Science **302**, 1188 (2003).S. Savel'ev, V. Misko, F. Marchesoni, and F. Nori, Phys. Rev. B **71**, 214303 (2005); V. R. Misko, S. Savel'ev, F. Marchesoni, and F. Nori, Physica C **426–431**, 147 (2005); F. Nori, Nat. Mater. **2**, 227 (2006).

[23] Y. Otani *et al.* (unpublished).

[24] K. J. Kirk, J. N. Chapman, S. McVitie, P. R. Aitchison, and C. D. W. Wilkinson, Appl. Phys. Lett. **75**, 3683 (1999).

[25] K. J. Kirk, J. N. Chapman, S. McVitie, P. R. Aitchison, and C. D. W. Wilkinson, Appl. Phys. Lett. **87**, 5105 (2000).

[26] K. J. Kirk, J. N. Chapman, and C. D. W. Wilkinson, J. Appl. Phys. **85**, 5237 (1999).

[27] R. P. Cowburn, J. Phys. D **33**, R1 (2000).

[28] M. Tsoi, R. E. Fontana, and S. S. P. Parkin, Appl. Phys. Lett. **83**, 2617 (2003).

[29] F. Cayssol, D. Ravelosona, C. Chappert, J. Ferré, and J. P. Jamet, Phys. Rev. Lett. **92**, 107202 (2004).

[30] Y. Yokoyama, Y. Suzuki, S. Yuasa, K. Ando, K. Shigeto, T. Shinjo, P. Gogol, J. Miltat, A. Thiaville, T. Ono, and T. Kawagoe, J. Appl. Phys. **87**, 5618 (2000).

[31] P. Bruno, Phys. Rev. Lett. **83**, 2425 (1999).

[32] A. Himeno, T. Okuno, S. Kasai, T. Ono, S. Nasu, K. Mibu, and T. Shinjo, J. Appl. Phys. **97**, 066101 (2005).

[33] T. Taniyama, I. Nakatani, T. Yakabe, and Y. Yamazaki, Appl. Phys. Lett. **76**, 613 (2000).

[34] S. Savel'ev, A. Rakhmanov, and F. Nori, New J. Phys. **7**, 82 (2005).

[35] Alex Hubert and Rudolf Schäfer, *Magnetic Domains: The Analysis of Magnetic Microstructures* (Springer, New York, 2001).

[36] M. Borromeo, P. Hänggi, and F. Marchesoni, J. Phys.: Condens. Matter **17**, S3709-S3718 (2005).

[37] C. Costantini and F. Marchesoni, Europhys. Lett. **48**, 491 (1999); P. Reimann, C. Van den Broeck, H. Linke, P. Hänggi, J. M. Rubí, and A. Perez-Madrid, Phys. Rev. Lett. **87**, 010602 (2001); F. Marchesoni, S. Savel'ev, and F. Nori, Europhys. Lett. **73**, 513 (2006); Phys. Rev. E **73**, 021102 (2006).

[38] L. Gammaitoni, P. Hänggi, P. Jung, and F. Marchesoni, Rev. Mod. Phys. **70**, 223 (1998); T. Wellens, V. Shatokhin, and A. Buchleitner, Rep. Prog. Phys. **67**, 45 (2004).

[39] S. Savel'ev, A. Rakhmanov, and F. Nori, Phys. Rev. E **72**, 056136 (2005).

[40] L. D. Landau, E. M. Lifshitz, and L. P. Pitaevskii, *Electrodynamics of Continuous Media* (Butterworth-Heinemann, Oxford, 1995).

[41] H. Kronmüller and D. Goll, Physica B **319**, 122 (2002).